J Mol Model (2004) 10:223–232
DOI 10.1007/s00894-004-0190-0

ORIGINAL PAPER

Kamil Sternal · Jacek Czub · Maciej Baginski

Molecular aspects of the interaction between amphotericin B and a phospholipid bilayer: molecular dynamics studies

Received: 1 August 2003 / Accepted: 9 March 2004 / Published online: 30 April 2004

Abstract Amphotericin B (AmB) is a polyene macrolide antibiotic used to treat systemic fungal infections. The molecular mechanism of AmB action is still only partly characterized. AmB interacts with cell-membrane components and forms membrane channels that eventually lead to cell death. The interaction between AmB and the membrane surface can be regarded as the first (presumably crucial) step on the way to channel formation. In this study molecular dynamics simulations were performed for an AmB–lipid bilayer model in order to characterize the molecular aspects of AmB–membrane interactions. The system studied contained a box of 200 dimyristoylphosphatidylcholine (DMPC) molecules, a single AmB molecule placed on the surface of the lipid bilayer and 8,065 water molecules. Two molecular dynamics simulations (NVT ensemble), each lasting 1 ns, were performed for the model studied. Two different programs, CHARMM and NAMD2, were used in order to test simulation conditions. The analysis of MD trajectories brought interesting information concerning interactions between polar groups of AmB and both DMPC and water molecules. Our studies show that AmB preferentially took a vertical position, perpendicular to the membrane surface, with no propensity to enter the membrane. Our finding may suggest that a single AmB molecule entering the membrane is very unlikely.

Keywords Amphotericin B · Molecular dynamics · Phospholipid membrane · DMPC · Molecular modeling

K. Sternal · J. Czub · M. Baginski (✉)
Department of Pharmaceutical Technology and Biochemistry,
Faculty of Chemistry,
Gdansk University of Technology,
Narutowicza St 11/12, 80-952 Gdansk, Poland
e-mail: maciekb@hypnos.chem.pg.gda.pl
Tel.: (+48)(583471596)

Introduction

Amphotericin B (AmB), Fig. 1, is a polyene macrolide anti-fungal antibiotic used in the treatment of systemic fungal infections. Despite its different undesirable side effects, in particular its nephrotoxicity, AmB is still the drug of choice used to treat serious infections due to the lack of better alternatives. [1, 2, 3, 4] The emerging problem of systemic fungal infections is a consequence of advanced medical treatment of patients (e.g., extensive use of antimicrobial antibiotics and anticancer chemotherapeutics) and impairment of the immune system caused by other factors (e.g., HIV infections). Therefore, the search for new anti-fungal drugs or the improvement of old standards is still an important challenge. [5, 6, 7] Unlike other anti-fungal drugs, amphotericin B exhibits several positive features: (i) high anti-fungal activity, (ii) wide anti-fungal spectrum, (iii) fungicidity, and (iv) low ability to generate resistance in fungal strains. [3, 8] For these reasons, a continuing effort is being made towards the design of less toxic derivatives of AmB. Our laboratory has also contributed to this effort, which has resulted in the synthesis of several active and less toxic derivatives of AmB. [9, 10]

The AmB molecule consists of a lactone ring and an aminosugar moiety connected via a glycosidic bond (Fig. 1). The so-called "polar head" of the molecule contains carboxyl and amino groups (Fig. 1) and due to the presence of these groups, AmB is a zwitterion under physiological conditions. Both carboxyl and amino groups are important for the chemotherapeutic activity/selectivity of the antibiotic and chemical modifications of one or both of these groups led to new derivatives of AmB. [9, 11, 12, 13, 14, 15] The lactone ring of AmB is a rather rigid and extended structure. It contains seven conjugated carbon–carbon double bonds in one part of the ring and a chain of hydroxyl groups, which are able to form intramolecular hydrogen bonds, in the other part of the ring. The AmB molecule thus exhibits amphiphilic properties. [16] These amphiphilic and amphoteric properties of AmB are responsible for the ability of the an-

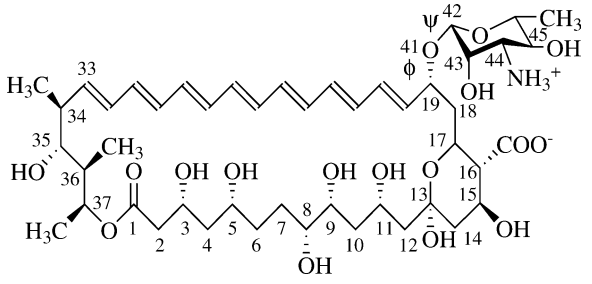

Fig. 1 The structure of the amphotericin B molecule with partial numbering of the heavy atoms referenced in the text

tibiotic molecules to form membrane channels [17, 18, 19] and different supramolecular complexes in water, [20, 21, 22] in a lipid environment or at the membrane surface [23, 24, 25] as well as on the air–water interface. [26, 27, 28, 29]

The complex molecular mechanism of action of AmB is still not well understood, which hampers all efforts to design new AmB derivatives with much improved chemotherapeutic properties. It is known that AmB molecules form ionic membrane channels that are lethal for fungal cells. [18, 23, 30] It is believed that chemotherapeutic application of AmB is based on the slightly higher affinity of the antibiotic towards ergosterol-containing membranes (fungal cells) than cholesterol-containing membranes (animal cells). [24, 31, 32] There are only minor differences in the chemical structure between cholesterol and ergosterol molecules and the reasons why ergosterol-containing membranes are better affected than cholesterol-containing ones are still poorly understood. The mechanism of action of AmB has been studied experimentally for several decades (e.g. [18, 23, 30, 32]). In addition to experimental efforts, theoretical studies using various computational chemistry methods have been carried out (e.g. [16, 33, 34, 35, 36, 37, 38, 39, 40, 41, 42]). Generally, three molecular factors responsible for the mechanism of AmB selective toxicity (which is higher against ergosterol than cholesterol containing membranes) are considered. Firstly, it is hypothesized that small structural differences between sterols are responsible for the higher stability of AmB–ergosterol than AmB–cholesterol channels. [43] Secondly, studies of the associated state of AmB (and its derivative MFAME [9]) in water revealed that this state of association influences the selective toxicity of the antibiotic. [44, 45, 46] Thirdly, the mode of interaction between AmB and phospholipid membranes and especially the different abilities of the antibiotic molecules to enter cholesterol- and ergosterol-containing membranes also influence the selective toxicity of AmB. [44]

The molecular aspects of interactions between AmB and the surface of a phospholipid membrane have been studied less than properties of membrane channels or the associated state of the antibiotic. Therefore, in our current work we specifically concentrated on the AmB–membrane surface interaction. Finding the mode of AmB–phospholipid interactions may help to understand the way AmB molecules enter the membrane and form different supramolecular complexes (including channels) within the membrane. Recently, it was postulated that AmB dimers, rather than monomers form AmB–membrane channels. [28, 29] To answer the question if monomers, dimers or higher associates of AmB are able to enter the membrane is also pivotal for understanding the mechanism of AmB channel formation. Two mechanisms have been proposed. First, the so-called "sequential mechanism", in which monomeric AmB molecules enter the cell membrane and then form channels. In this case the antibiotic molecules may interact with sterols or other lipids and form complexes prior to channel formation. Since AmB molecules form monolayers at the air–water interface, another mechanism of channel formation called the "one step" mechanism assumes that AmB may also form aggregates on the membrane surface. These higher associates formed on the membrane surface may enter the membrane in one step and form the channel. Whether the "sequential" or "one step" mechanism leads to membrane-channel formation is important from the therapeutic point of view and may help in the design of AmB derivatives that will act more selectively towards fungal versus mammalian cells.

In our work, we present molecular dynamics studies of a single AmB molecule interacting with a phospholipid membrane built of dimyristoylglycerophosphatidylcholine (DMPC) molecules. [47] Progress in molecular modeling methods as well as developments in computer technology have made it possible to study large systems such as lipid bilayers and lipid-interacting ligands at the atomic level. [48, 49, 50] To the best of our knowledge, no molecular modeling simulation of AmB interactions with membrane models has ever been performed. We are aware that rather short MD simulation (in our case 1 ns) is not long enough to observe an AmB molecule entering the membrane. Therefore, the aim of our work was to characterize and analyze the molecular factors governing interactions between AmB and a lipid bilayer, especially to analyze which groups of AmB are involved in this interaction and what is the dynamic behavior of the antibiotic on the membrane surface. Such an analysis may help to find out if a single molecule of AmB exhibits any propensity to enter the lipid membrane. Our present work is the first simulation of a series in which interactions between AmB (monomer or dimer) and a membrane (surface or interior) are studied and analyzed.

Methods

The system simulated contained 200 DMPC molecules (100 molecules in each layer), one AmB molecule and 8,065 water molecules. A fully equilibrated starting membrane structure (a box of fully hydrated bilayer of phospholipids) was taken, with the author's permission, from Zubrzycki et al. [47] The dimensions of this starting box were: 7.8 nm×7.8 nm×6.4 nm. The amphotericin B molecule was placed horizontally on the membrane surface, with its longest molecular axis perpendicular to the bilayer normal (in this case the *z*-coordinate). Afterwards, a layer of 2,582 water molecules was added to solvate the antibiotic molecule entirely. All molecular mechanics and molecular dynamics (MD) calculations

described herein employed a force-field parameter set for phospholipids from CHARMM ver. 28b1. [51] The exception was the set of AmB site charges which was taken from previous MD simulations. [43, 52] These charges were obtained by fitting to the electrostatic potential generated by the antibiotic molecule. [16]

Three energy minimization steps were carried out for our system. Firstly, the water layer, which was added at the beginning, was subjected to 3,000 steps of energy minimization using the conjugate gradient method; during this process all other atoms were kept fixed. The structure obtained was then subjected to a further 3,000 steps of energy minimization using the conjugate gradient method. In this process, the top layer of water molecules (containing the AmB molecule) was allowed to move freely, except for the AmB molecule itself. Finally, the entire system was subjected to 3,000 steps of energy minimization using the same gradient method as before. These minimization procedures allowed extra water and AmB molecules, which were added to the original equilibrated box of phospholipids, to relax.

Two molecular dynamics simulations with distinct simulation parameters were carried out—simulations (I) and (II). A time step of 2 fs and the SHAKE routine were used in both simulations. We also used two molecular dynamics trajectory integrators: one was the CHARMM package [53] (simulation I) and the second the NAMD2 program [54] (simulation II). Both simulations involved an NVT ensemble (constant number of particles N=8266, volume V, and temperature T=300 K), although the boundary conditions were different in the two simulations.

The simulation submitted to the CHARMM program, simulation (I), involved using a constraining plane potential of 1.25 kJ mol^{-1} nm^{-2} (originally in the CHARMM program 30 kcal mol^{-1} $Å^{-2}$) to ensure constant volume of the model. It is worth mentioning that this constraining plane potential was asymmetric and may be regarded as a border potential active only when selected atoms were beyond the defined box. Atoms affected by this potential in simulation (I) included: the oxygen of the waters (for x=±3.9 nm, y=±3.9 nm, z=4.25 nm, and z=−3.0 nm) and the following atoms for DMPC: choline nitrogen, phosphorus atom, C1 atom of the glycerol residue and carbon atoms number 6, 12, 14 from the Sn1 and Sn2 chains (for x=±4.1 nm, y=±4.1 nm). Unfortunately, it was not possible to impose a border potential for all atoms of the selected molecules because the number of constrained atoms in the system reached the program limit. The border potential was also applied for AmB. In pilot molecular dynamics simulations, without a border potential for AmB, the AmB molecule not only took a vertical position with regard to the membrane but also tried to escape from the box after breaking contact with the surface of the membrane. In order to keep AmB in the simulated box, carbon atoms number 33, 38, 39, 40 and the oxygen atom of the hydroxyl group at carbon C38 (for z=4.25 nm) were also added to this list. This potential for AmB operated such that it was switched on when the molecule was outside the box and switched off when it was inside. Thus, the border potential for AmB did not influence the behavior of the AmB molecule inside the box (e.g. its propensity to adopt horizontal or vertical positions).

In simulation (II), carried out with NAMD2, periodic boundary conditions using fixed dimension of unit cell (i.e., 7.8 nm× 7.8 nm×7.4 nm) were employed for all molecules in the system.

The choice of two MD simulations with an NVT ensemble and different boundary conditions was directly linked to the phospholipid model chosen and the ability to treat the whole system in terms of CPU time. The box of phospholipids (containing 200 lipid molecules) used in our work belongs to the largest phospholipid systems ever simulated within an all atom approach. This all atom approach is important in our case because in the future we plan to perform MD simulations with the antibiotic molecules immersed in the membrane. The united atom approach widely used in MD simulations of lipid membranes is very efficient in terms of CPU time but may not be an appropriate approach to monitor weak interactions between lipid chains and amphiphilic molecules such as AmB present inside the membrane. The all atom approach was used in the work of Zubrzycki et al. [47] and for the sake of consistency we followed the same path. Two NVT simulations were chosen because application of constant V enabled us to control the area per lipid molecule. In simulation (II) this area was kept the same as in the simulation performed by Zubrzycki et al. [47] (i.e., 0.608 nm^2), in a very good agreement with the experimental values. [55] On the other hand, the area per lipid molecule was kept slightly larger in simulation (I) (i.e., 0.672 nm^2). This was in order to give the AmB molecule more freedom to interact with different groups of the polar phospholipids (e.g., phosphorus groups). In contrast to simulation (II), in the simulation (I) a periodic boundary condition was not applied. This was in order to test if it is possible to skip the very CPU demanding periodic boundary conditions for such a large system when one would like to observe only interactions of the ligand (placed in the center of the lipid surface) with the lipid membrane. Choosing one simulation without periodic boundary conditions enforced the application of cut-offs for long range non-bonded interactions. To be consistent, cut-offs and not the more popular Ewald sums, Particle Mesh Ewald or Fast Multipoles methods were also applied to treat long-range electrostatic interactions in simulation (II). This approach may have introduced some shortcomings, which are discussed later, but on the other hand was consistent with the work of Zubrzycki et al., [47] in which cut-offs were used.

Thus in both simulations the cut-off method was used to calculate Lennard-Jones and electrostatic interactions. For simulation (I), a cut-off distance of 1.4 nm was used for Lennard-Jones and Coulombic interactions. A switching function at a distance of 1.1 nm was used to separate the short-range portion of the electrostatic interactions from the long-range component. The same values were used in simulation (II). The equilibration process was performed for both simulations before data collection in the final simulation. In the case of simulations (I) and (II), the equilibration lasted 100 ps and 55 ps, respectively. The total energy of the system was monitored and the equilibration time was sufficient to obtain energy convergence for the structures studied. Moreover, it is worth recalling that the starting DMPC box was already equilibrated [47] so only short equilibration was necessary after adding AmB and some water molecules. The productive MD run lasted 1.1 ns for simulation (I) and 1.0 ns for simulation (II). The non-bonded pair list of atoms was updated every 25 steps in simulation (I) and every 20 steps in simulation (II). The frames were collected every 2 ps.

Results and discussion

Two molecular dynamics simulations, lasting around 1 ns (see Methods), were performed for the system studied and two MD trajectories were collected. Our analysis of the MD simulation data focused on the intermolecular and the intramolecular structural and dynamical properties of AmB, DMPC and the water molecules that define/characterize interactions between the antibiotic molecule and the phospholipid membrane. We were also interested in differences between the two trajectories that may be useful from the methodological point of view in preparing studies of similar systems in the future.

Intramolecular properties of AmB

Because of the presence of seven conjugated C=C double bonds, the lactone ring of AmB is quite rigid. However, a *trans–gauche* flip is possible in a fragment containing hydroxyl groups—especially in the region between the C5 and C8 carbon atoms—where the uniform configuration of the polyhydroxyl chain is altered (Fig. 1). Such conformational changes have already been observed in MD simulation of AmB's membrane channel. [41] In the present work, we also found such conformational *trans–gauche* flips for the C6–C7 carbon bond (Fig. 2).

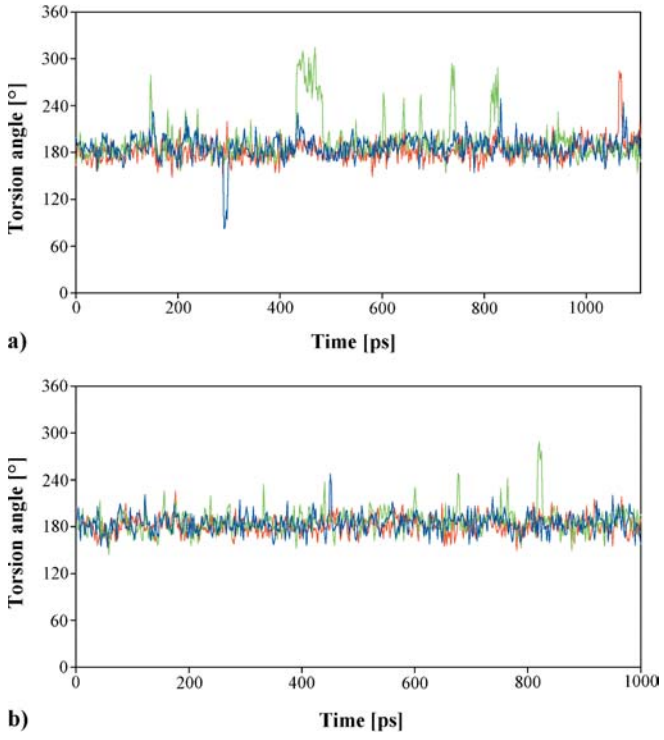

Fig. 2 Change of the dihedral angles along the polyhydroxyl chain in the AmB lactone ring as a function of time. *Blue*—dihedral angle defined by C4–C5–C6–C7 atoms; *green*—dihedral angle defined by C5–C6–C7–C8 atoms; *red*—dihedral angle defined by C6–C7–C8–C9 atoms. **a** Simulation (I). **b** Simulation (II)

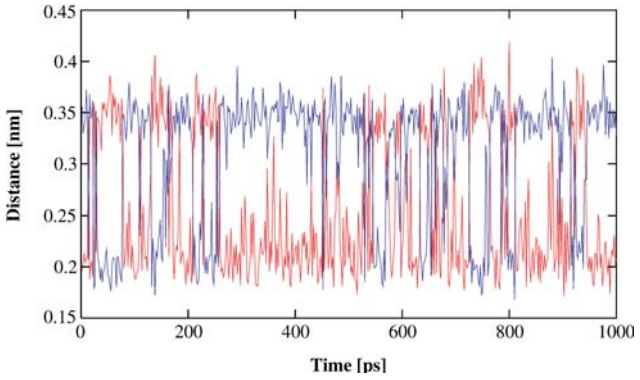

Fig. 3 The distance between the hydrogen atom of the hydroxyl group at C3 (AmB) and the neighboring oxygen-atom acceptors: *red*—the AmB's carbonyl group at C1; *blue*—the AmB's hydroxyl group at C5. The data are shown only for simulation (I). The interchange of the hydrogen bonds is easily observed when one superimposes the two curves

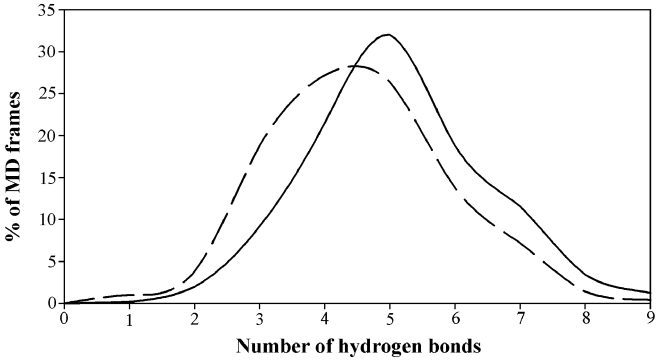

Fig. 4 Distribution of the total number of intramolecular hydrogen bonds in the AmB molecule: simulation (I)—*solid line*; simulation (II)—*dashed line*

However, this conformational change was unstable and the *gauche* conformation returned to *trans* after less than 50 ps.

Amphotericin B contains several hydroxyl groups in the lactone ring. These can interact with water or amino groups of DMPC molecules. On the other hand, the same hydroxyl groups can form intramolecular hydrogen bonds with each other. Therefore, analysis of the intramolecular hydrogen bonds was performed for AmB. We were particularly interested in the hydroxyl groups at AmB's carbon atoms C3, C5, C9, C11 and C13. All these hydroxyl groups form intramolecular hydrogen bonds that are interchangeable between neighboring partners. For instance, the hydrogen atom of the hydroxyl group at C11 can potentially form a hydrogen bond either with the hydroxyl group at carbon atom C9 or at C13. In Fig. 3, an example of such an interchange is shown. Figure 3 shows data for the simulation (I) but similar changes were observed in both simulations. The hydrogen atom of the hydroxyl group at carbon C3 forms a hydrogen bond with either the hydroxyl group at carbon atom C5 or with the neighboring carbonyl group (see Fig. 1 for location of atoms). However, a different situation was observed for the hydroxyl group at carbon atom C11. In this case, fewer exchanges were recorded and it was found that the hydrogen atom from the hydroxyl group at C11 interacts preferentially with the hydroxyl group at carbon atom C9 (data not shown). The total distribution of intramolecular hydrogen bonds for AmB is shown in Fig. 4. In both simulations, AmB preferentially formed more than five intramolecular hydrogen bonds.

Another important intramolecular feature of AmB is the mutual positions of the aminosugar moiety and the lactone ring. This conformation, defined by φ (C18–C19–O41–C42), ψ (C19–O41–C42–C43) dihedral angles, determines the overall shape of the antibiotic molecule and the ability of the carboxyl and amino groups of AmB to form either intramolecular or intermolecular hydrogen bonds. Rotations around bonds C19–O41 and O41–C42 were traced and a φ, ψ map is shown in Fig. 5. Only two conformers were found but one of them (φ=270°, ψ=180°) is much more populated than the second (φ=210° ψ=180°). It is worth mentioning that the location of the aminosugar moiety (with regard to the lactone ring), observed in this study in free AmB is different from that in the AmB molecules within the channel structure. [43] In the channel structure the two conformers are equally populated, especially when the AmB–ergosterol channel is considered. [43] The difference may stem from the fact that, in the channel structure, sterols can interact with a

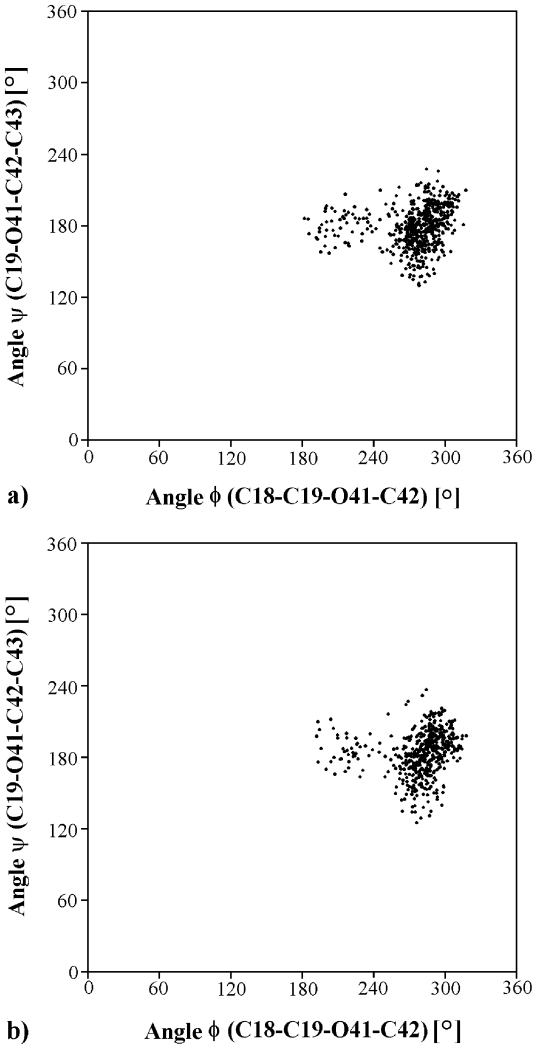

Fig. 5 Distribution of φ and ψ dihedral angles defining the relative position of the lactone ring and the aminosugar moiety of AmB. Each dot corresponds to one MD frame. **a** Simulation (I); **b** Simulation (II)

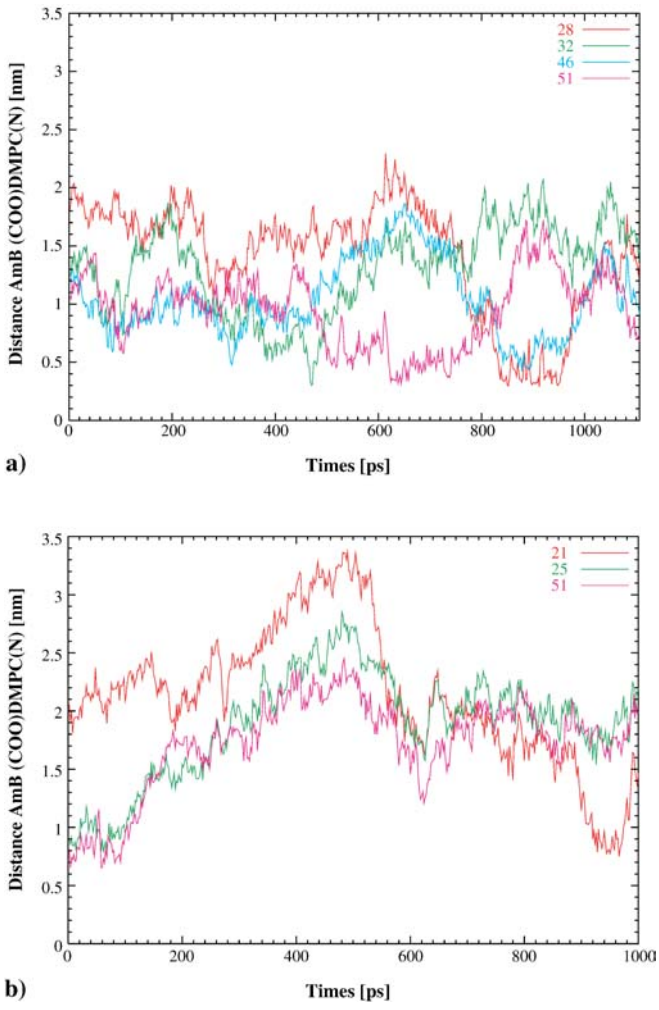

Fig. 6 The distance between the carbon atom of AmB's carboxyl group and the nitrogen atom of the neighbor DMPC's amino groups monitored in time. In simulation (I), only DMPC, for which the traced distance was lower than 0.5 nm, was selected—panel **a**. In simulation (II) only the two closest DMPC molecules are shown—panel **b**. Numbers of the interacting DMPC molecules are shown in the upper right corner of each panel

polar head of the AmB molecules and these interactions could drive changes in the position of the aminosugar moiety. On the other hand, in our system the dihedral angles φ, ψ may also be influenced by the interaction of the amino group of AmB with the phosphate groups of DMPC. However, in both simulations (I and II) only weak interactions of this type were observed. For a short period of time (about 20 ps) in the simulation (I) the distance between AmB's nitrogen atom and DMPC's phosphorus atom was found to be shorter than 0.5 nm.

The final remark in this section concerns the system of conjugated C=C double bonds. It was mentioned that seven conjugated C=C carbon bonds enforce rigidity of the AmB lactone ring. However, due to its length, the polyene fragment itself is not strictly planar and bends to some extent (data not shown). Such behavior was also observed in the previous molecular dynamics studies of AmB, both in the channel structure and with a free AmB molecule in water. [41, 56]

Intermolecular properties of AmB

The major objective of the simulation performed was to analyze the interactions between AmB and the phospholipid membrane. To this end, several molecular parameters were monitored; one of them was the distance between the carboxyl group of AmB and the amino group of DMPC molecules (Fig. 6). The second parameter was the distance between the amino group of AmB and the phosphate groups of DMPC molecules (Fig. 7). It is worth underlining that interactions between the groups mentioned are mostly electrostatic and of ionic character because all these groups are ionized. The recorded distance shown in Fig. 6 is defined as that between the carbon atom in AmB's carboxyl group and the nitrogen atom in DMPC's amino group. In the case of simulation (I), a strong interaction (short distance) between AmB and DMPC was found for at least four DMPC molecules (Fig. 6a). The threshold value of 0.5 nm for this distance

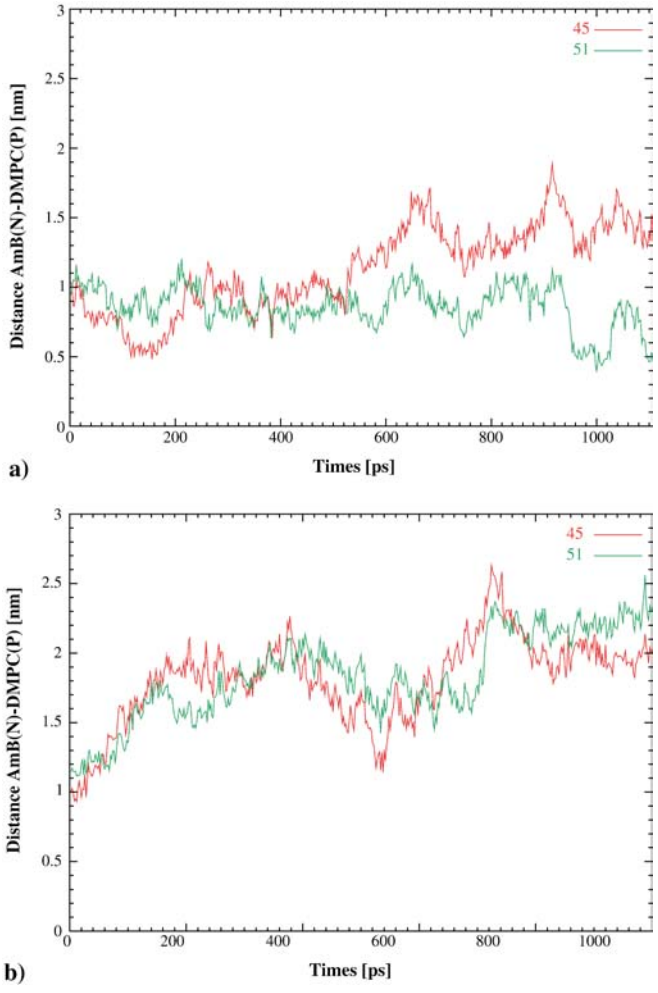

Fig. 7 The distance between the nitrogen atom of AmB's amino group and the phosphorus atom of the neighboring DMPC's phosphate groups. No threshold distance was used and only two of the closest DMPC molecules were selected. **a** Simulation (I); **b** Simulation (II). Numbers of the interacting DMPC molecules are shown in the upper right corner of each panel

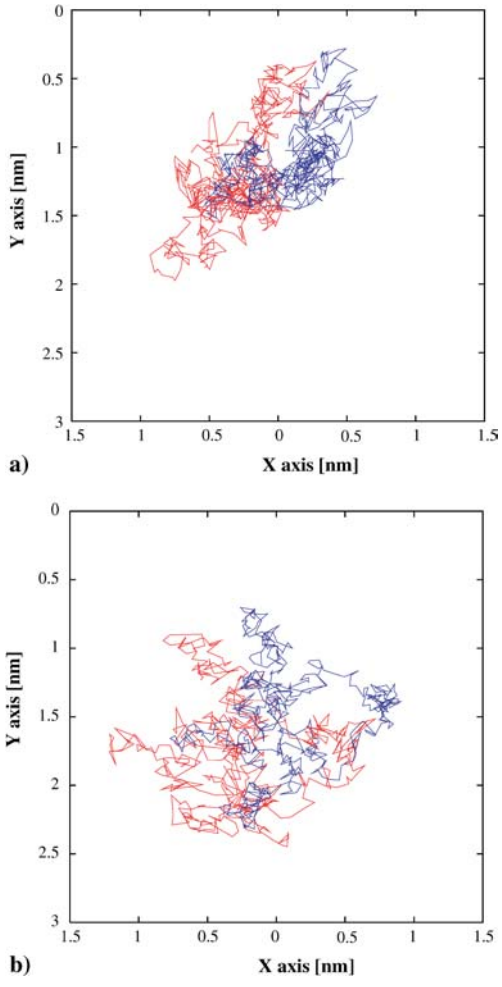

Fig. 8 Trajectory of the nitrogen atom (*blue line*) and the carbon atom (*red line*) from AmB's amino and carboxyl groups, respectively, projected on the *XY* plane. **a** Simulation (I). **b** Simulation (II)

was chosen to show the interaction between AmB and DMPC since the value chosen corresponds to an almost van der Waals contact of the two molecules. The recorded distance shown in Fig. 7 is defined as that between the nitrogen atom in AmB's amino group and the phosphorus atom in DMPC's phosphate group. DMPC's phosphate groups are located below the average level of DMPC's amino groups in the membrane, so in our case longer distances were expected. However, no threshold value was used for this distance and only the distance between AmB and two nearest DMPC molecules is shown in Fig. 7. When analyzing the data in Figs. 6 and 7, one may find a substantial difference between simulations (I) and (II). In simulation (I), much better contact between the AmB molecule and DMPC molecules was found than in the simulation (II). This finding is in agreement with other molecular parameters monitored in the two simulations, which are discussed later in this section.

The stronger interactions between AmB and DMPC molecules found in the simulation (I) are also supported by the data in Fig. 8 which shows a projection of the MD trajectory of AmB's amino group (the nitrogen atom) and the carboxyl group (the carbon atom) on the *XY* plane. This projection shows, in some way, the lateral diffusion of the AmB on the membrane surface. In the case of simulation (I) (Fig. 8a) the trace of both AmB's groups is much more focused than in the case of simulation (II) (Fig. 8b). It was also found that the AmB molecule in simulation (II) tends to stay horizontal during the whole simulation (data not shown). On the other hand, the position of the AmB molecule in the simulation (I) is to some extent vertical (Fig. 9). This observation is in agreement with the experimental data, showing that at the water–air interface AmB itself forms monolayers or monolayer structures with lipids. [26, 27] Our simulation supports this observation, showing that the vertical position of AmB on the lipid surface is preferred. At this point it is interesting to note the difference between simulations (I) and (II) concerning the position of AmB. One may suppose that a driving force for the vertical position of AmB was its

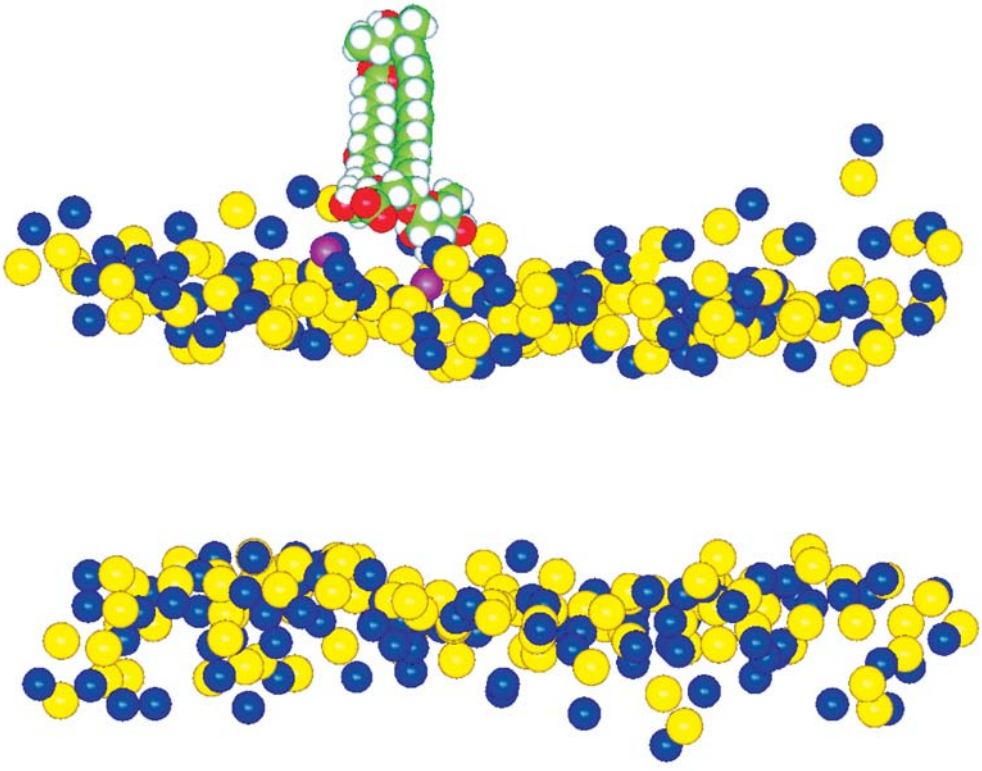

Fig. 9 A simple snapshot from MD simulation (I) (frame caught at time 850 ps) showing the semi-vertical position of AmB with regard to the membrane surface. For the sake of clarity, only the AmB molecule and the DMPC's nitrogen (*blue balls*) and phosphorus (*yellow balls*) atoms are shown. Two phospholipids, DMPC numbers 28 and 51 (see also Fig. 6a), interacting with the AmB molecule are highlighted in *magenta*. The following colors were used for atoms in AmB: *green*—carbon, *blue*—nitrogen, *red*—oxygen, *white*—hydrogen

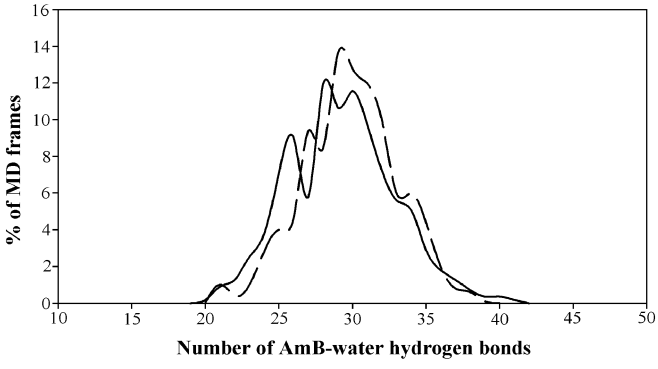

Fig. 10 Distribution of the number of intermolecular hydrogen bonds between AmB and water molecules: simulation (I)—*solid line*; simulation (II)—*dashed line*

strong interaction with DMPC molecules. Periodic boundary condition and the more compact structure of the lipid bilayer (smaller area per one lipid in the simulation (II) compared to simulation (I)—see later) in the case of the simulation (II) may be the reason that a strong AmB–DMPC interaction was not encountered in 1 ns of the simulation (II). On the other hand, DMPC and the water molecules had more freedom in simulation (I) and this might be a reason that this strong AmB–DMPC interaction occurred and, in consequence, even in a 1-ns simulation the vertical position of AmB was recorded. All these observations point out that boundary conditions (especially the size of the lipid box in the *XY* plane) and freedom of the molecules in the system are very important for the behavior of such long and rather rigid molecule as AmB at the membrane surface.

Another property analyzed during our studies was solvation of AmB by water. In this case, the number of hydrogen bonds formed between water molecules and all donor and acceptor atoms of AmB was traced. The distribution of AmB–water hydrogen bonds is shown in Fig. 10. A pair of groups was assumed to be hydrogen bonded if the distance between acceptor and donor atoms was shorter than 0.35 nm and the plane angle formed by donor–hydrogen–acceptor atoms was larger than 90°. In both simulations, the position of the maximum in the distribution curve was very similar. These data show that AmB forms about 30 hydrogen bonds with the surrounding water molecules. Thus, the antibiotic molecule is well solvated. The correlation between the number of hydrogen bonds formed by AmB and its ability to interact with DMPC molecules is also worth noting. The number of hydrogen bonds formed by AmB (AmB is an acceptor in this case) as a function of time is shown in Fig. 11. The lower number of the hydrogen bonds formed between AmB and water molecules at 650–750 ps (Fig. 11a) correlates with a stronger interaction between AmB and DMPC molecules (Fig. 6).

Properties of the phospholipids bilayer

In order to analyze interactions between AmB and the surface of the membrane, the intra- and intermolecular properties of the phospholipids were also monitored and analyzed in our MD simulation.

A deuterium order parameter, S_{CD}, an experimental quantity, is the quantity very often calculated for phos-

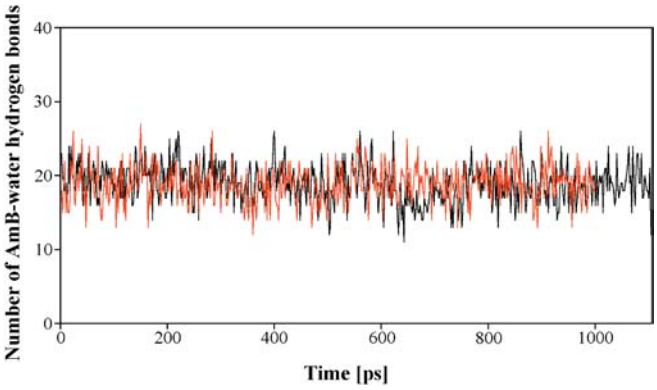

Fig. 11 Number of intermolecular hydrogen bonds between AmB (as an acceptor) and water molecules (as donors) monitored in time: simulation (I)—*black*; simulation (II)—*red*

pholipid molecules to validate the bilayer interior. In our case this parameter was calculated according to Eq. (1):

$$S_{\mathrm{CD}} = \left\langle \frac{3}{2}\cos^2\Theta - \frac{1}{2} \right\rangle \qquad (1)$$

Angle Θ is the angle between the C–H bond vector (in particular for methylene groups of DMPC the fatty-acid chain) and the bilayer normal (Z direction). The brackets in the equation denote an averaging over all lipids and over time. In our case, the averaging was performed only over all DMPC molecules in the upper layer, i.e. the ones that could potentially interact with the AmB molecule. The calculated order parameters S_{CD} (data not shown) were compared with the experimental values obtained for DMPC [57] and DPPC. [58] The values of S_{CD} obtained in simulation (II) are in a very good agreement with the experimental data. On the other hand, the S_{CD} values calculated in simulation (I) are lower (i.e., lipids are less ordered). This difference may stem from the dimension of the phospholipid box, which was slightly different in the two simulations. However, the order parameters obtained in both simulations are consistent with the area per lipid, i.e., smaller area higher order and vice versa.

Another feature that was monitored in both simulations was the solvation pattern of the DMPC molecules. As shown before, [59] polar heads of the phospholipid molecules are well solvated by water molecules, which are able to form hydrogen bonds with phospholipids and to form chains of water bridges between DMPC molecules. Therefore, we traced the total number of hydrogen bonds between the DMPC molecules (all heteroatoms able to form hydrogen bonds were included) and the water molecules. In both simulations, this average value of DMPC–water hydrogen bonds per DMPC molecule is about seven.

The atomic density along the bilayer normal (Z axis) of some selected atoms of DMPC and water molecules was monitored as a measure of the distribution of certain groups within the membrane. The electron density (X-ray or neutron diffraction) was measured experimentally for phospholipid membranes and the distribution profiles of atoms or electrons derived from our simulations can therefore be compared with these experimental values (see e.g., [60]). In our case, the nitrogen and phosphorus atoms of the DMPC molecules and the oxygen atom of the water molecules were included in our calculation of the atom-density profile across the membrane (data not shown). It was found that, in the case of simulation (I), the bilayer is thinner (Z coordinate) than that obtained in simulation (II). The thickness of the membrane measured as the P–P distance (defined by the positions of the phosphorus atoms in two bilayers) was found to be around 3.0 nm and 3.8 nm in simulations (I) and (II), respectively. The differences found for the two simulations may stem from the slightly different size (XY cross-section) of the simulation box of phospholipids used in the MD simulations. In the case of simulation (I), the applied boundary potentials gave more freedom to the DMPC molecules. As a result, an average area per lipid molecule could reach values up to 0.672 nm^2 in simulation (I) versus 0.608 nm^2 in simulation (II). The latter value is closer to experimental values reported previously, which range between 0.595 nm^2 and 0.652 nm^2. [60]

Concerning the interaction between AmB and DMPC molecules, no large difference between the two simulations was found. When the interaction of the ligand with the surface of the phospholipid bilayer is studied, one may suggest that more attention should be paid to parameters defining the membrane interface (e.g., area per lipid). In the case of simulations of ligands inside the membrane, parameters defining the interior of the bilayer should be better reproduced (e.g., S_{CD} parameter and thickness). In our case, the area per lipid was fixed (NVT ensemble) and close to the experimental value. Therefore, simulation (II) may be considered as a reasonable representation of ligand–membrane interactions.

Conclusions

The amphotericin B molecules form channels in the membrane and interaction of AmB with the surface of the membrane is an important part of the antibiotic chemotherapeutic action. Because of the amphiphilic and amphoteric properties of AmB, the molecules of this antibiotic form different supramolecular structures in water and lipid environments. The ability of a single AmB molecule to enter the membrane has been proposed to be a factor responsible for the lower toxicity of the antibiotic. [44] It was found that single molecules of AmB (not associates) are not able to penetrate membranes that contain cholesterol. [44] The ability to enter the membrane by a single AmB molecule may also indicate that AmB–channel formation in the membrane occurs sequentially.

Our present work is the first attempt to simulate the interaction between AmB and a membrane surface, specifically phospholipids. To the best of our knowledge, it is the first report presenting molecular dynamics studies of interactions between AmB and a phospholipid membrane.

Two simulations of 1 ns were performed for the system containing one AmB molecule, 200 DMPC molecules and 8,065 water molecules. There were no sterol molecules in our model system but more complex models are being considered for future studies. The aim of our work was to analyze interactions between AmB and the lipid bilayer, to observe the dynamic behavior of AmB on the surface as well as to find out if a single molecule of AmB exhibits any propensity to enter the membrane. Based on the data obtained from the molecular dynamic simulation, several conclusions can be drawn.

Intramolecular properties of AmB

AmB forms intramolecular hydrogen bonds between those parts of AmB molecule that contain hydroxyl groups. Only two preferred mutual positions of the lactone ring of AmB and the aminosugar moiety are found. Since only one of them is highly populated in the AmB molecules involved in the channel structure, [43] one may postulate that this intramolecular property is important for supramolecular complex formation by the AmB molecules and their derivatives. The intramolecular dynamic behavior of the AmB molecule found in our simulations is similar to that found in previous studies. [41, 56, 61]

Intermolecular properties of AmB

Interaction of AmB with the membrane and the dynamic behavior of AmB on the membrane surface were analyzed carefully and no tendency of the AmB molecule to enter the membrane was found. On the contrary, AmB is able to take a vertical position with regard to the membrane surface. Such an orientation helps the AmB molecule to interact with the membrane and enables AmB's polar head to interact with a polar head of the DMPC molecules. Such interactions were recorded in particular between the carboxyl group of AmB and the amino group of DMPC. Since these interactions last for about 100 ps, one may assume that, once formed, the AmB–DMPC complex diffuses in the *XY* plane of the membrane. This observation agrees with the ability of the AmB to form monolayers at the air–water interface. [26, 27] One may even propose that a single AmB molecule cannot enter the membrane because other AmB molecules are necessary to form a monolayer or other supramolecular structure on surface of the membrane. In this case, supramolecular complexes of the AmB molecules formed on the membrane surface can reorganize further in order to enter the membrane and eventually to form the channel. Such supramolecular structures containing many AmB molecules were recently observed by atomic force microscopy on the membrane surface [25] and suggested based on spectroscopic data in water. [22] Thus, our molecular dynamics studies support the idea that a single AmB molecule is not able to enter a lipid membrane containing only phospholipids. However, further simulations (including both AmB monomers and dimers) are necessary to clarify whether AmB behaves similarly in membranes containing sterols.

Comparison of the two simulation (NVT ensemble) revealed that both of them reproduced molecular parameters of the phospholipid membrane reasonably well but in the case of studies on ligands embedded in the membrane (future projects) the NPT ensemble will be more suitable.

Acknowledgments The authors acknowledge financial support by the State Committee for Scientific Research, Warsaw (Poland), grant number 6P05F00321, and by Gdansk University of Technology, internal grant. We would like to thank the Computational Center TASK, Gdansk (Poland) for granting CPU time on their mainframe machines. We also would like to thank Ms. Malgorzata Grabska (former diploma student) for help in setting up pilot simulations at the early stages of this project.

References

1. Gallis HA, Drew RH, Pickard WW (1990) Rev Infect Dis 12:308–329
2. Hartsel S, Bolard J (1996) Trends Pharmacol Sci 17:445–449
3. Ghannoum MA, Rice LB (1999) Clin Microbiol Rev 12:501–517
4. Ablordeppey SY, Fan PC, Ablordeppey JH, Mardenborough L (1999) Curr Medicinal Chem 6:1151–1195
5. Bastert J, Schaller M, Korting HC, Evans EGV (2001) Int J Antimicrobial Agents 17:81–91
6. De Pauw BE (2000) Int J Antimicrobial Agents 16:147–150
7. Tiphine M, LetscherBru V, Herbrecht R (1999) Transplant Infect Dis 1:273–283
8. VandenBossche H, Dromer F, Improvisi I, LozanoChiu M, Rex JH, Sanglard D (1998) Med Mycol 36:119–128
9. Grzybowska J, Sowinski P, Gumieniak J, Zieniawa T, Borowski E (1997) J Antibiot 50:709–711
10. Cybulska B, Kupczyk K, Szlinder-Richert J, Borowski E (2002) Acta Biochim Pol 49:67–75
11. Mechlinski W, Schaffner CP (1972) J Antibiot 25:256–258
12. Wright JJ, Albarella JA, Krepski LR, Loebenberg D (1982) J Antibiot 35:911–914
13. Jarzebski A, Falkowski L, Borowski E (1982) J Antibiot 35:220–229
14. Falkowski L, Jarzebski A, Stefanska B, Bylec E, Borowski E (1980) J Antibiot 33:103–104
15. Czerwinski A, Konig WA, Zieniawa T, Sowinski P, Sinnwell V, Milewski S, Borowski E (1991) J Antibiot 44:979–984
16. Baginski M, Borowski E (1997) Theochem J Mol Struct 389:139–146
17. de Kruijff B, Demel RA (1974) Biochim Biophys Acta 339:57–70
18. Hartsel SC, Hatch C, Ayenew W (1993) J Liposome Res 3:377–408
19. Fujii G, Chang JE, Coley T, Steere B (1997) Biochemistry 36:4959–4968
20. Mazerski J, Bolard J, Borowski E (1982) Biochim Biophys Acta 719:11–17
21. Barwicz J, Gruszecki WI, Gruda I (1993) J Colloid Interface Sci 158:71–76
22. Millie P, Langlet J, Berges J, Caillet J, Demaret JP (1999) J Phys Chem B 103:10883–10891
23. Bolard J (1986) Biochim Biophys Acta 864:257–304
24. Fournier I, Barwicz J, Tancrede P (1998) Biochim Biophys Acta 1373:76–86
25. Milhaud J, Ponsinet V, Takashi M, Michels B (2002) Biochim Biophys Acta 1558:95–108
26. Seoane JR, Vila Romeu N, Minones J, Conde O, Dynarowicz-Latka P, Casas M (1997) Progr Colloid Polym Sci 105:173–179
27. Minones J, Carrera C, Dynarowicz-Latka P, Conde O, Seoane R, Patino JMR (2001) Langmuir 17:1477–1482
28. Gagos M, Koper R, Gruszecki WI (2001) Biochim Biophys Acta 1511:90–98
29. Gruszecki WI, Gagos M, Kernen P (2002) FEBS Lett 524:92–96

30. Brajtburg J, Powderly WG, Kobayashi GS, Medoff G (1990) Antimicrob Agents Chemother 34:183–188
31. Teerlink T, De Kruijff B, Demel RA (1980) Biochim Biophys Acta 599:484–492
32. Kerridge D (1986) Adv Microb Physiol 27:1–72
33. Bonilla-Marin M, Moreno-Bello M, Ortega-Blake I (1991) Biochim Biophys Acta 1061:65–77
34. Meddeb S, Berges J, Caillet J, Langlet J (1992) Biochim Biophys Acta 1112:266–272
35. Khutorsky VE (1992) Biochim Biophys Acta 1108:123–127
36. Langlet J, Berges J, Caillet J, Demaret JP (1994) Biochim Biophys Acta 1191:79–93
37. Mazerski J, Borowski E (1996) Biophys Chem 57:205–217
38. Khutorsky V (1996) Biophys J 71:2984–2995
39. Baginski M, Gariboldi P, Borowski E (1994) Biophys Chem 49:241–250
40. Baginski M, Bruni P, Borowski E (1994) Theochem J Mol Struct 311:285–296
41. Baginski M, Resat H, McCammon JA (1997) Mol Pharmacol 52:560–570
42. Resat H, Sungur FA, Baginski M, Borowski E, Aviyente V (2000) J Comput Aid Molec Design 14:689–703
43. Baginski M, Resat H, Borowski E (1999) Biophys J 76:M-Pos531
44. Bolard J, Legrand P, Heitz F, Cybulska B (1991) Biochemistry 30:5707–5715
45. Cybulska B, Gadomska I, Mazerski J, Grzybowska J, Borowski E, Cheron M, Bolard J (2000) Acta Biochim Pol 47:121–131
46. Szlinder-Richert J, Mazerski J, Cybulska B, Grzybowska J, Borowski E (2001) Biochim Biophys Acta 1528:15–24
47. Zubrzycki IZ, Xu Y, Madrid M, Tang P (2000) J Chem Phys 112:3437–3441
48. Feller SE (2000) Curr Opin Colloid Interface Sci 5:217–223
49. Forrest LR, Sansom MSP (2000) Curr Opin Struct Biol 10:174–181
50. Saiz L, Klein ML (2002) Acc Chem Res 35:482–489
51. Feller SE, Mackerell AD (2000) J Phys Chem B 104:7510–7515
52. Baginski M, Resat H, Borowski E (2002) Biochim Biophys Acta 1567:63–78
53. Brooks BR, Bruccoleri RE, Olafson BD, States DJ, Swaminathan S, Karplus M (1983) J Comput Chem 4:187–217
54. Kale L, Skeel R, Bhandarkar M, Brunner R, Gursoy A, Krawetz N, Phillips J, Shinozaki A, Varadarajan K, Schulten K (1999) J Comput Phys 151:283–312
55. Petrache HI, Tristam-Nagle S, Nagle JF (1998) Chem Phys Lipids 95:83–94
56. Mazerski J, Borowski E (1995) Biophys Chem 54:49–60
57. Urbina JA, Moreno B, Arnold W, Taron CH, Orlean P, Oldfield E (1998) Biophys J 75:1372–1383
58. Douliez JP, Leonard A, Dufourc EJ (1996) J Phys Chem 100:18450–18457
59. Pasenkiewicz-Gierula M, Takaoka Y, Miyagawa H, Kitamura K, Kusumi A (1997) J Phys Chem A 101:3677–3691
60. Nagle JF, Tristram-Nagle S (2000) Curr Opin Struct Biol 10:474–480
61. Anachi RB, Bansal M, Easwaran KRK, Namboodri K, Gaber BP (1995) J Biomol Struct Dyn 12:957–970